Paper for AIAA 2nd Meet. & Tech. Demonstration, July 26-29, 1965, San Francisco, Calif. (Entry Veh. Session)

GENERALIZED ABLATION ANALYSIS WITH APPLICATION TO HEAT-SHIELD MATERIALS AND TEKTITE GLASS

By Fred W. Matting* and Dean R. Chapman**

National Aeronautics and Space Administration
Ames Research Center
Moffett Field, California

INTRODUCTION

The development of heat shields for space vehicles and long-range missiles has motivated a marked increase in the effort to understand the process of ablation. This intensified study is contributing to the understanding of natural ablative phenomena that occur when extraterrestrial bodies enter the Earth's atmosphere. Ablation data obtained in the laboratory, particularly in arc-jet wind tunnels, do not duplicate in any single experiment all the conditions of entry flights; hence, there is need for analytical methods of predicting and explaining the ablative phenomena. Before such methods can be applied, however, their validity and accuracy must be determined by comparing calculated results with results from wind-tunnel tests, with flight data, or with post-flight observations of a man-made or natural object when one can be recovered.

A generalized method is presented here for solving the problem of stagnation-point heat transfer and material response for blunt bodies experiencing melting and vaporizing or subliming ablation. An attempt has been made to describe the problem mathematically as completely as possible in order to obtain nearly exact solutions. This required that the analysis be machine programmed for numerical solutions. This program in various stages of development has been used successfully at the Ames Research Center during the past three years. It has previously been employed in the analysis of tektite ablation.[14,17]

Many things incorporated in the analysis are already well established; however, some of the features are new. The analysis takes account of the fact that entry bodies initially fly in the free-molecule regime, then in a transitional regime, and finally

---

*Research Scientist
**Staff Scientist

in the continuum regime of gas dynamics. The analysis contains formulas for the transitional regime to bridge the free-molecule and continuum regimes; these formulas have been rationally derived from simple models and are believed to be new.

Several options in the analysis and associated computing program are available. Internal radiation in the body is accounted for, or the body can be assumed to be opaque. Flight cases as well as wind-tunnel cases can be calculated; the flight cases can be applied to any planet provided certain characteristics of the atmosphere are known. Material properties and external flow conditions can be arbitrarily put into the program so that a wide variety of ablation research problems can be studied.

To illustrate the types of problems presently being handled and to elucidate significant ablative phenomena, several examples are presented.

Example calculations are given of the ablation of tektite-glass models in an arc-heated wind tunnel when heating is constant and ablation is mainly by melting; calculated values of surface recession and surface brightness temperature are compared with experiment. As an example of the ablation of a substance that both melts and vaporizes, an entry flight into the Earth's atmosphere of an opaque tektite is calculated. The calculated depth of penetration of aerothermal stresses is compared with that measured on recovered tektites. An example is calculated for the entry into the Earth's atmosphere of a vehicle with a silica glass heat shield (which both vaporizes and melts). The heat shield was considered as a transparent and as a semitransparent glass; the results of the two calculations are compared with the known amount of ablation. Two examples are given for the ablation of Teflon, a material that undergoes a surface depolymerization to the vapor state (a process which thus resembles sublimation). One of the examples is for a series of Teflon models ablating in an arc-heated wind tunnel at constant heating conditions; calculated values of surface recession are compared with measured values. The other example for Teflon is that of the entry of a small vehicle into the Martian atmosphere; in this example, the effect of the uncertain knowledge of the atmospheric scale height for Mars is examined.

ANALYSIS

The analysis summarized below contains a number of established equations and familiar approximations that have been used by previous investigators.[1-4] The familiar forms will not be discussed in any detail, but new or novel features of the analysis will be presented and only briefly discussed since a detailed discussion is beyond the scope of the present paper.

Basic Approach and Approximations

The analysis is concerned with the problem of surface ablation near the stagnation point for transparent or opaque materials of finite thickness. The analysis is thus restricted to materials that undergo surface ablation including melting, evaporation, sublimation, or surface chemical reactions, such as depolymerization. Chemical reactions involving the external gases are not considered. The boundary-layer equations, as such, are not solved, but results of known solutions are used to obtain heating rates, surface shear, and the effects of mass transfer. Heating rates must be solved for, in order to determine the front and back face boundary conditions. The heating environments treated are generally of two types. One is of constant velocity and stream density, such as generally exists in an arc-heated wind tunnel. The other environment is with time-varying velocity and density over an entry flight (using a constant lift/drag ratio but a variable mass). In this latter environment, the equations of motion are solved simultaneously with the heat transfer and ablation equations. In the equations of motion, the quantity M/C_DA appears, and this is related (empirically) to the surface recession.

Conservation Equations

The analysis is essentially a time-dependent energy balance along the stagnation center line of an axisymmetric blunt body. The basic equations to be solved are the conservation equations for energy, mass, and momentum, written in a simplified form that is valid near the stagnation center line. The energy and momentum equations have been further simplified by neglecting inertial terms, which is a valid approximation for viscous ablative materials such as glass, stone, or any subliming material.

The curvilinear coordinate system used is shown in the sketch,

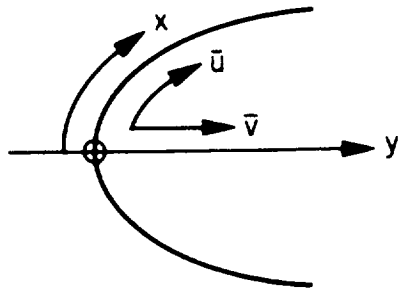

The conservation equations are:

$$\text{Energy} \qquad \rho c_p \left(\frac{\partial T}{\partial t} + \bar{v} \frac{\partial T}{\partial y} \right) = \frac{\partial}{\partial y} \left[K \frac{\partial T}{\partial y} - F(y,t) \right] \tag{1}$$

where $F(y,t)$ is the internal radiation flux term.

$$\text{Continuity (for constant density)} \qquad \frac{\partial \bar{u}}{\partial x} + \frac{\bar{u}}{x} + \frac{\partial \bar{v}}{\partial y} = 0 \tag{2}$$

$$\text{x-Momentum} \qquad \frac{\partial}{\partial y} \left(\mu \frac{\partial \bar{u}}{\partial y} \right) = \frac{\partial p}{\partial x} - \frac{\rho a x}{R} \tag{3}$$

Most previous analyses have taken account of internal radiation or vehicle acceleration, but not both. The acceleration term in the momentum Eq. (3) can be important in determining the rate of removal of melted material; this term, as written, is valid in the stagnation region.

In the evaluation of the internal radiative flux, F, we assume either an opaque body ($F \equiv 0$) or a transparent gray body (two shades of gray; one for the incoming gas cap radiation, another for the absorption-emission of the heat-shield material). A third alternative is to approximate the transparent gray body by a semitransparent body that is opaque internally but has a variable surface emissivity. The evaluation of the radiative flux for the gray transparent body is similar to that of Ref. 5 which treats scattered radiation and uses an exponential attenuation. The present evaluation employs the second-degree exponential integral,[6] E_2, and considers one reflection from the front and the rear surfaces, which is a good approximation for materials that absorb well.

$$\frac{F(y,t)}{2n^2\alpha\sigma} = \int_0^y T(\eta)^4 E_2[\alpha(y-\eta)]d\eta - \int_y^{y_{BF}} T(\eta)^4 E_2[\alpha(\eta-y)]d\eta + R_{eff}\int_0^{y_{BF}} T(\eta)^4 \{E_2[\alpha(y+\eta)]$$

$$- E_2[\alpha(2y_{BF} - (y+\eta))]\}d\eta + \frac{q_R}{2n^2\alpha\sigma}\left[e^{-\alpha_2 y} - R_{eff}e^{-\alpha_2(2y_{BF}-y)}\right] \tag{4}$$

where R_{eff} is the effective coefficient of reflection for planar radiation.[7] The gas cap radiation has been evaluated empirically as

$$q_R = E_4 R D^{E_5} V^{E_6} \tag{5}$$

to fit existing data, where E_4, E_5, and E_6 are input constants for a given environment, and V is the "enthalpy velocity" (see Nomenclature). In the calculation for the semi-transparent body, the surface emissivity is varied in an appropriate manner with the thickness of the temperature profile (thermal thickness). This variation is derived by assuming an exponential temperature distribution near the wall. It gives virtually the same results for most ablation characteristics as the transparent case (see Table I), although the internal temperature profiles do not agree closely. It greatly reduces computing machine time, however; hence it is used for most calculations where an accuracy of the order of 10 percent is adequate.

Boundary Conditions

The boundary conditions on Eq. (1) are determined in the standard manner by writing surface energy balances for the front and back surfaces, providing for the appropriate differences between the opaque and transparent cases. Options are provided in determining the rear surface boundary conditions. For heat-shield calculations, a sink with an arbitrarily selected heat capacity is used to back up the heat shield. For small body or tektite calculations, a base heating rate is employed that is related to the front surface heating rate. It is noted that the surface temperatures generally cannot be specified a priori, as these depend partly on external conditions which may be changing with time. The computing program must "find" the appropriate boundary conditions that satisfy the partial differential Eq. (1) and the surface energy balances.

Method of Solution

The method of solution of the system of Eqs. (1-3) is first to solve the momentum Eq. (3) by a numerical quadrature, to obtain $\bar{u}$. One inserts $\bar{u}$ into the continuity Eq. (2), and by another numerical quadrature $\bar{v}$ is obtained. Then one puts $\bar{v}$ into the energy Eq. (1), and this equation is solved by finite differences. A forward difference scheme is employed in a manner similar to previous investigations.[1-4] To take account of the decreasing depth of material with time, a shrinking coordinate system is used, so that the number of grid points remains constant.

The environment acting on the ablator will either be constant or time varying. For wind-tunnel calculations, the external conditions imposed on the ablator will be known, and will usually be constant. For flight cases, we use the two-dimensional trajectory equations (with variable mass) for entry in a meridional plane for the time-varying external conditions acting on the ablator.[8] Thus the flight case solves simultaneously the conservation equations of mass, momentum, and energy for the ablating material, the appropriate aerodynamic boundary conditions, and the trajectory equations of flight motion.

A number of physical properties of the ablation material which appear in the analysis (e.g., thermal conductivity, specific heat, viscosity) are functions of temperature. These functions have been represented analytically, with constants in the representations that can be read into the numerical computing program. For example, viscosity is represented by

$$\mu = e^{\frac{B_4}{T-B_{14}} - B_5} \tag{6}$$

where B_4, B_5, and B_{14} are the input constants for a given material.

The accuracy of solutions obtained by the finite-difference method will depend on the grid spacings in time and space. As a semi-independent check on the accuracy obtained, a running energy balance is computed. A residual (error) based on energy rates is obtained, and a cumulative residual based on total energies is calculated. These energy balances also, as illustrated later, show the dispositions of the energies involved.

The Free-Molecule, Continuum, and Transition Regimes

In order to write the forward surface energy balance, one needs to know the convective heat transfer at the surface. In laminar continuum flow we can evaluate the surface convective heat transfer as[9] (with a vorticity correction)

$$q_{oc} = \frac{A_4 \sqrt{D}\, V^{1.15}}{\sqrt{R}} \left(V^2 - 0.00836\, \bar{c}_p T_w\right)\left(1 + \frac{C_6}{\sqrt{DVR}}\right) \tag{7}$$

where A_4 is a constant and $\bar{c}_p$ contains constants that depend on the planetary atmospheric composition, C_6 is a vorticity correction (generally small), and V is the "enthalpy velocity." Equation (7) gives excellent agreement with existing experimental data over an extended range of enthalpy potentials. The value of A_4 for Earth entries is approximately 1.1; in wind-tunnel tests, A_4 is evaluated with a calorimeter. With a blowing correction we have

$$q_{\psi c} = \psi q_{oc} \tag{8}$$

where we evaluate ψ as

$$\psi = \frac{0.94}{1 + \dfrac{B_{11}}{\left[\left(\dfrac{p_{t_2}}{p_v}\right)^{E_7} - 1\right]\left(1 + \bar{v}_{ch}\right)}} + 0.06 \tag{9}$$

This relation gives a good fit to a number of boundary-layer solutions.[10-12] The exponent E_7 (normally unity) accounts for suppression of vaporization by the presence of oxygen.[13] The constants E_7 and B_{11}, of course, will vary with material and composition of the planetary atmosphere. The correction term, $\bar{v}_{ch} = \bar{v}_{wc}/\bar{v}_{wFM}$, is zero except for surface chemical reactions when it accounts for possible rate control (see Nomenclature). For surface convection in the free-molecule regime we use a Newtonian approximation

$$q_{FM} = \frac{A_{cq} D V_\infty}{0.0836} \left(V^2 - 0.00836\, \bar{c}_p T_w\right) \tag{10}$$

In the transition regime between free-molecule and continuum flow, the convective heat transfer will have a value bridged between the evaluations in Eqs. (8) and (10). This has been rationally derived from a simple kinetic theory model. The details of the derivation are beyond the scope of the present paper, but the result turns out to be

$$q_{\psi w} = q_{\psi c}\left[1 - e^{-(q_{FM}/q_{\psi c})}\right] \tag{11}$$

Equation (11) is an example of several new features of the analysis and its associated computing program. In Ref. 14 a purely empirical free-molecule-continuum bridging formula was used. Both Eq. (11) and the empirical formula give good fits to existing data, but Eq. (11) is now being used because it has a theoretical basis. Similar bridging formulas for surface shear and surface normal velocity are noted below. Bridging formulas are needed for some wind-tunnel conditions and for entry flights of small bodies, such as tektites. During an entry flight, a tektite, for example, will pass through the free-molecule, transitional, and continuum regimes. Using an expression such as Eq. (11) automatically takes account of these changes of heating rates.

In the quadrature of the momentum Eq. (3), we need the x-derivative of the surface shear. In the continuum regime, this quantity, τ'_{wc}, is evaluated using a modified Reynolds analogy with a correction for blowing as given in Ref. 11. In the free-molecule regime, the x-gradient of surface shear, τ'_{wFM}, is evaluated by a Newtonian approximation and is unaffected by blowing. Using a model similar to that used for heat transfer, we obtain (from a derivation outside the scope of this paper) the bridging relation for the x-derivative of surface shear

$$\tau'_w = \tau'_{wc}\left[1 - e^{-(\tau'_{wFM}/\tau'_{wc})}\right] \tag{12}$$

Equation (12) is new, and it replaces previously used empirical forms. In passing through the free-molecule, to transitional, to continuum regimes, formula (12) will automatically take account of the changes in surface shear.

The normal front-face velocity, $\bar{v}_w$, is needed in the quadrature of the continuity Eq. (2) and in the front surface heat balance. The value of this quantity depends on

surface and external conditions. For the diffusion controlled regime, we calculate $\bar{v}_{wd}$ using the so-called Lewis analogy (Le = 1), which states that the ratio of mass diffusion to concentration "gradient" is equal to the ratio of continuum heat transfer to enthalpy potential.[15] For the free-molecule or rate-controlled regime, we distinguish two cases: (1) evaporation or sublimation for which we have the Langmuir equation, and (2) a chemical reaction, such as a depolymerization, for which we use an Arrhenius type rate equation. The bridging or transitional formula between the two regimes, valid for evaporation, sublimation, or chemical reactions, is:

$$\frac{1}{\bar{v}_w} = \frac{1}{\bar{v}_{wFM}} + \frac{1}{\bar{v}_{wd}} \tag{13}$$

The use of Eq. (13) automatically places the velocity in the appropriate regime: the diffusion-controlled, the rate-controlled, or the transitional regime.

Example Derivation of Bridging Equation: Transition Between Free-Molecule and Diffusion-Controlled Regimes for Front-Face Normal Velocity

As an example to illustrate the type of bridging we are using, we briefly outline the derivation of Eq. (13) for $\bar{v}_w$ for the evaporation case. The Langmuir equation in its usual form for the free-molecule regime can be written

$$\dot{m}_{FM} = A_{cv} p_v \sqrt{\frac{m_v}{2\pi R_g T}} \tag{14}$$

We define p_a as the actual vapor pressure as distinguished from the equilibrium vapor pressure, p_v. We have, then, for the actual mass loss rate

$$\dot{m} = (p_v - p_a) A_{cv} \sqrt{\frac{m_v}{2\pi R_g T}} \tag{15a}$$

$$\dot{m} = \dot{m}_{FM} \left(1 - \frac{p_a}{p_v}\right) \tag{15b}$$

The mass transfer by diffusion is essentially proportional to p_a, but the theoretical maximum diffusion rate is

$$\dot{m}_d = K_d p_v \tag{16}$$

so we can write

$$\dot{m} = \dot{m}_d \left(\frac{p_a}{p_v}\right) \tag{17}$$

With a quasi-steady state assumption, we can say that the mass loss by rate control is diffused away at the same rate, so we can eliminate p_a/p_v between Eqs. (15b) and (17) and obtain

$$\frac{1}{\dot{m}} = \frac{1}{\dot{m}_{FM}} + \frac{1}{\dot{m}_d} \tag{18}$$

Cancelling out the constant density, ρ, we have Eq. (13). A similar derivation for the evaporation case is to be found in Ref. 16. These forms (Eqs. (13) and (18)) are considered valid over the complete spectrum from rate control to diffusion control and are also valid for the chemical reaction case. The other bridging equations ((11) and (12)), listed above, are similarly derived from simple models. The only bridging equation for the transitional regime which has not been derived from a simple model is that for the coefficient, C_D, which appears in the trajectory equations and which has been bridged empirically to fit existing data.

ILLUSTRATIVE RESULTS

The examples shown below represent several types of ablation. Calculated and measured results are compared for all examples except the last one, which is a Martian entry. The dispositions of energies for the examples given are summarized in table I.

Tektite Glass in a Wind Tunnel

Tektite glasses, ablated at high enthalpies in an arc-jet wind tunnel, furnish examples of ablators that both vaporize and melt. Typical comparisons between calculated and measured values of surface recession and surface brightness temperature are shown in Figs. 1 and 2. The agreements can be seen to be very good, which lend confidence that flight cases involving tektite glass can be successfully calculated.[14] In both figures the calculations were made for a transparent glass and for a semitransparent glass, and there is little difference between the results of the two methods of computation. The glasses used in these examples ablate by melting more than by vaporization because of the

moderate enthalpy in the wind tunnel, the low viscosities, and low vapor pressures of the glasses. For the glasses in Fig. 1, about one percent of the ablation is due to vaporization, and for the glasses in Fig. 2, vaporization accounts for less than one percent. At higher enthalpies the relative amount of vaporization increases. In table I is shown the disposition of energies calculated for the semitransparent glass of Fig. 1. Due to the small amount of vaporization, very little heat is blocked, and most of the incoming energy is accounted for by melting.

Tektite Entry Calculation

The results of calculations for a typical opaque tektite entry case are shown in Figs. 3 and 4. An entry speed of 11.0 km/sec and an entry angle of -30° were used for the calculations. These conditions correspond to a typical deduced trajectory for a Victoria australite (Ref. 17, Fig. 22). In Fig. 3 are shown calculated values of velocity, surface temperature, surface recession, and surface recession due to vaporization. The free-molecule and continuum regimes are also distinguished. Time zero is arbitrarily selected as "far out" before any appreciable aerodynamic heating has begun. This example illustrates the response of a material that vaporizes readily, with about 14 percent of the ablation due to vaporization and the rest from melting. As the tektite heats up, its surface begins to ablate at a temperature in excess of 2000° K. The surface temperature and ablation rate reach a maximum and then fall off as the body slows down. The end of ablation occurs rather abruptly, and the remainder of the flight is that of a solid body being aerodynamically cooled. Measurements of the amount of ablation at the stagnation point[14,17] on recovered tektites yield values not greatly different than the 7.3 mm calculated for this example. The calculations indicate that for this flight, a negligible portion of the ablation occurred in the free-molecule regime. The portion of the ablation in the transitional regime was 24 percent, compared to the majority of ablation in the continuum regime (76 percent). For smaller tektites and shallow entry angles the percent of ablation in the free-molecule and transitional regimes will be greater; for large vehicles this portion of ablation is generally small.

In Fig. 4 are shown variations of the calculated temperature profiles and surface recession with time. This figure gives a fairly complete picture of the internal heating and eventual cooling of the body during its flight. Measurements on recovered bodies show locked in thermal stresses that vary from a depth of 0.2 cm to a depth of 0.35 cm, corresponding to the calculated depth of 0.23 cm.[17] The post-flight observations of thermal stresses and deduced surface recession on recovered bodies are compatible with the calculated results. The energy dispositions for the flight calculated are in table I. The vaporization that occurs in this flight causes substantial heat blockage; the bulk of the energy is accounted for by heat blockage, heating and vaporizing, and heating and melt flow, these three quantities being of about the same order of magnitude.

Reentry Flight With Silica Glass Heat Shield

A calculation was made for a reentry flight of a nose-cone with an opaque silica glass heat shield. This vehicle and flight are described by Hidalgo and Kadanoff.[18] For this trajectory and this heat-shield material the portion of ablation due to vaporization is about 14 percent which is comparable to the tektite entry case previously discussed. The recovered reentry vehicle allowed the amount of ablation, X, at the

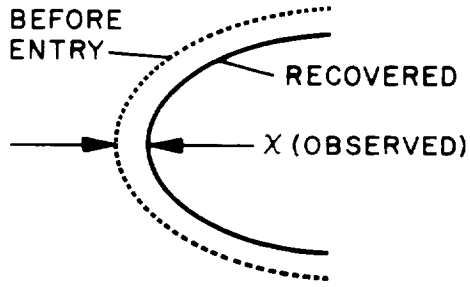

stagnation point to be determined. The physical-property inputs in this case correspond to opaque silica,[18] but both the transparent and the semitransparent options of the computing program were run with the results

$$\frac{X\ (\text{transparent})}{X\ (\text{observed})} = 1.11 \qquad \frac{X\ (\text{semitransparent})}{X\ (\text{observed})} = 1.15$$

The corresponding ratio as calculated by Hidalgo and Kadanoff using their quasi-steady ablation analysis was about 1.10 and by Chapman and Larson[14] using a different (integral) method of calculation, 0.92. This illustrates that the amount of ablation on simple

materials such as glass can be computed to the order of 10- to 15-percent accuracy by several methods, including two of the options of the present program. In view of the inevitable angle-of-attack variations in flight, which cause the stagnation point of maximum heating to wander somewhat over the nose and thus reduce somewhat the maximum recession, the observed difference between calculated and measured ablation is in the expected direction. The energy dispositions for both the transparent and semitransparent calculations are shown in table I. It is of interest that the two calculations yield energy proportions that are nearly the same, although the internal temperature distributions are different because of radiative transmission in the transparent case. In both cases the total ablation is moderate, so that the actual amount of vaporization is moderate and the heat blockage term is relatively small.

Teflon Model in an Arc-Jet Wind Tunnel

Under normal ablative conditions, tetrafluoroethylene polymer (Teflon) undergoes a surface depolymerization and vaporization of the monomer at a surface temperature of approximately 760° K. There is no one specific temperature at which the reaction occurs, but a sharply rising reaction rate with temperature in this neighborhood essentially controls the surface temperature of an ablating model.[19,20] Under these conditions, the viscosity of Teflon remains high, so the process can be said to resemble a sublimation (with the reaction rate determined by an Arrhenius type rate equation). In performing the calculations for Teflon ablation, it was assumed that any energy involved in possible chemical reactions between the Teflon vapor and the external gases could be neglected.

Comparisons between calculated and experimentally measured surface recession for Teflon are shown in Fig. 5. The experiments by G. Lee and R. Sundell, Ames Research Center, (unpublished) were performed in an arc-jet wind tunnel for four values of enthalpy. It is seen that the agreement obtained is quite good with the possible exception of the 700 Btu/lb total enthalpy case. It is thought that the generally satisfactory agreement shown in the figure indicates the validity of the method of calculation and also that the physical properties of the substance have been adequately represented.

The dispositions of the calculated energies for the 2000 Btu/lb total enthalpy case are shown in table I. The heat blockage term is fairly large, because all the ablated material leaves in the vapor state. The largest term is the energy for heating, depolymerizing, and vaporizing.

Teflon Heat Shield in a Mars Entry

The calculations for this example illustrate entry for a proposed Mars probe.[21] A spherical capsule of 61.0-cm diameter has been assumed, with a 1-cm-thick Teflon heat shield, entering the Martian atmosphere in an oriented attitude. Four possible atmospheres have been assumed as tabulated below.

Composition (vol.)	Scale height, km
100% N_2	7.8
91% N_2, 9% CO_2	7.8
100% N_2	20.0
91% N_2, 9% CO_2	20.0

Calculations were made for an entry velocity of 7.92 km/sec and for two entry angles, -90° and -20°. An M/C_DA for continuum flow of 3.91 g/cm^2 was assumed for the vehicle, and M/A was held constant while the C_D varied through the transition from the free-molecule to the continuum regimes.

The -90° entries have the greatest peak-heating rates, but the -20° entries absorb the most total heat and are the most critical cases from a heat-shield standpoint. The heat-shield responses are compared using stagnation-point recession values as tabulated below.

Atmosphere	Entry angle	Total stagnation point recession, cm
N_2 small-scale height	-90°	0.098
N_2 large-scale height	-90°	.159
N_2-CO_2 small-scale height	-90°	.121
N_2-CO_2 large-scale height	-90°	.179
N_2-CO_2 small-scale height	-20°	.196
N_2-CO_2 large-scale height	-20°	.341

As seen by comparing the -90° entry cases in the table above, the most severe environment is with the mixed atmosphere and the large-scale height. The time of exposure to heating

is roughly proportional to scale height for two otherwise similar trajectories, and the total heat absorbed is approximately proportional to the square root of exposure time (and therefore scale height). This approximate relationship between scale height and total recession can be deduced from the table above. The strong dependence of the heat-shield response on the uncertainty of knowledge of the atmospheric scale height is considered to be important, as it will presumably apply to any heat-shield material.

The disposition of energies for the -20° case with large-scale height is shown in table I. As with the Teflon wind-tunnel results, the two large energy terms are the heat blockage term and the term that acounts for heating, depolymerizing, and vaporizing. In the environment of the -20° Martian entry, the considerable amount of ablation of material to the vapor state accounts for the very large heat blockage term.

The analysis has also been used in an approximate manner to calculate the quantities of interest around the front hemisphere of the spherical capsule for the most severe -20° entry case. The results are summarized in Fig. 6 which shows the variation of total recession and front and back face maximum temperatures around the hemispheric heat shield as well as the total mass loss. These results illustrate how variable material thickness may be used in heat-shield design.

CONCLUDING REMARKS

A generalized analysis of stagnation-point ablation has been presented for solving a wide variety of problems involving melting and vaporizing, subliming, or surface chemical reactions. The flexibility of the analysis has been demonstrated through the presentation of several varied illustrative examples. In general, it is expected that accuracy of answers obtained will depend largely on the degree of knowledge of the physical, chemical, and thermodynamic properties of the ablating material, as these are necessary inputs into the computing program. The procedure of relating calculations for a given material to experiment wherever possible has been noted. This gives confidence in calculations for the same material exposed to other conditions, when the response cannot be verified by experiment or observation. The analysis has been put into a numerical computing program written in IBM FORTRAN II.

NOMENCLATURE

a	y-direction body force per unit mass, cm/sec^2 (acceleration in flight case)
A	frontal area, cm^2
A_{cq}, A_{cv}	free-molecule accommodation coefficients for heat transfer, mass loss, dimensionless
A_4	constant, defined by Eq. (7)
B_{11}	constant, defined by Eq. (9)
c_p	specific heat, cal/g ^oK
$\bar{c}_p$	average specific heat, external gas, cal/g ^oK
C_D	drag coefficient (continuum), dimensionless
C_6	vorticity correction in Eq. (7)
D	free-stream density, g/m^3
$E_2(\eta)$	exponential integral[6]
E_7	constant, defined in Eq. (9)
F	radiation flux, cal/cm^2 sec
h_s	stagnation enthalpy, cal/g, J/kg, or Btu/lb, as specified
K	thermal conductivity, cal/cm sec ^oK
K_d	defined in Eq. (16)
Le	Lewis number, dimensionless
m	molecular weight
$\dot{m}$	mass loss rate, g/cm^2 sec
M	mass of body, g
n	index of refraction, dimensionless
p	pressure, dynes/cm^2 or atm, as specified
p_{t_2}	pressure downstream of normal shock, atm
p_v	equilibrium vapor pressure, atm
q_{oc}	surface convective (continuum) heat transfer with no blowing, cal/cm^2 sec
q_{oi}	initial surface convective heat transfer with no blowing, cal/cm^2 sec, W/cm^2, or Btu/ft^2 sec, as specified

q_{FM}	surface convective (free molecule) heat transfer, cal/cm^2 sec
q_R	gas cap radiation rate, cal/cm^2 sec
$q_{\psi c}$	surface convective (continuum) heat transfer with blowing, cal/cm^2 sec
$q_{\psi w}$	surface convective heat transfer (all regimes), cal/cm^2 sec
R	nose radius, cm
R_{eff}	effective coefficient of reflection for planar radiation, dimensionless
R_g	universal gas constant, ergs/mole ^oK
t	time, sec
T	temperature, ^oK
T_b	brightness temperature (emissivity unity), ^oK
$\bar{u}$	velocity in x-direction, cm/sec
$\bar{v}$	velocity in y-direction, cm/sec
$\bar{v}_{ch}$	$\bar{v}_{wc}/\bar{v}_{wFM}$ for surface chemical reactions only; otherwise zero (Eq. (9))
V	enthalpy velocity, km/sec; defined as $V^2 = 0.00836\ h_s$
V_∞	free-stream velocity, km/sec
x	longitudinal coordinate along meridian, cm
y	transverse coordinate normal to surface (inward), cm
α	absorption coefficient, internal radiation, cm^{-1}
α_2	absorption coefficient, gas cap radiation, cm^{-1}
γ	trajectory angle, deg
η	dummy variable, cm (Eq. (4))
μ	viscosity, poise
ρ	density (constant), g/cm^3
σ	Stefan constant, 1.369×10^{-12} cal/cm^2 sec $^oK^4$
τ	shear, dynes/cm^2
χ	surface recession, cm
χ_{vap}	surface recession due to vaporization, cm
ψ	convective heat blockage factor (Eq. (8)), dimensionless

Subscripts

a	actual (Eqs. (15) and (17))
BF	back face
c	continuum
d	diffusion
FM	free molecule
i	initial
max	maximum
s	stagnation (or settling chamber)
v	vapor expelled
w	wall (front face)
wc	wall, continuum
wd	wall, diffusion
wFM	wall, free molecule
o	no blowing
∞	free stream

Superscript

'	x-derivative

REFERENCES

[1]Landau, H. G., "Heat conduction in a melting solid," Quart. Appl. Math., 8, no. 1, 81-94 (April 1950).

[2]Lotkin, Mark, "The calculation of heat flow in melting solids," Quart. Appl. Math., 18, no. 1, 79-85 (April 1960).

[3]Fledderman, R. G., and Hurwicz, H., "Transient ablation and heat-conduction phenomena at a vaporizing surface," AVCO Tech. Rep. RAD TR-9(7)-60-9.

[4]Adams, Ernst W., "Theoretical investigations of the ablation of a glass-type heat protection shield of varied material properties at the stagnation point of a reentering IRBM," NASA TN D-564 (1961).

[5]Kadanoff, Leo P., "Radiative transport within an ablating body," ASME Jour. of Heat Transfer, 83, no. 2, 215-225 (May 1961).

[6]Kourganoff, V., "Basic methods in transfer problems," Clarendon Press, Oxford (1952).

[7]Gardon, Robert, "A review of radiant heat transfer in glass," J. Am. Ceramic Soc., 44, no. 7, 305-312 (July 1961).

[8]Chapman, Dean R., "An approximate analytic method for studying entry into planetary atmospheres," NASA TR R-11 (1959).

[9]Detra, R. W., Kemp, N. H., and Riddell, F. R., "Addendum to heat transfer to satellite vehicles reentering the atmosphere," Jet Propulsion, 27, no. 12, 1256-1257 (Dec. 1957).

[10]Hoshizaki, H., "Mass transfer and shock generated vorticity," ARS Jour., 30, no. 7, 628-634 (July 1960).

[11]Spalding, D. B., "The theory of melting ablation, with vaporization, gas phase chemical reaction, surface pyrolysis, and transient effects," Aeron. Quart., 12, pt. 3, 237-274 (Aug. 1961).

[12]Reshotko, Eli, and Cohen, Clarence B., "Heat transfer at the forward stagnation point of blunt bodies," NACA TN 3513 (1955).

[13]Hidalgo, Henry, "Ablation of glassy material around blunt bodies of revolution," ARS Jour., 30, no. 9, 806-814 (Sept. 1960).

[14]Chapman, Dean R., and Larson, Howard K., "On the lunar origin of tektites," J. Geophys. Res., 68, no. 14, 4305-4358 (July 1963).

[15]Eckert, E. R. G., and Drake, Robert M., Jr., "Heat and mass transfer," McGraw-Hill, N. Y. (1959).

[16]Scala, S. M., and Vidale, G. L., "Vaporization processes in the hypersonic laminar boundary layer," International J. Heat and Mass Trans., 1, no. 1, 4-22 (June 1960).

[17]Chapman, Dean R., "On the unity and origin of the australasian tektites," Geochim. et Cosmochim. Acta, 28, no. 6, 841-880 (June 1964).

[18]Hidalgo, Henry, and Kadanoff, Leo P., "Comparison between theory and flight ablation data," AIAA J., 1, no. 1, 41-45 (Jan. 1963).

[19]Wentink, Tunis, Jr., "High temperature behavior of Teflon," Avco-Everett Res. Rep. 55, AF BMD-TN-59-15 (1959).

[20]Madorsky, Samuel L., "Thermal degradation of organic polymers," Interscience Pub., N. Y. (1964).

[21]Seiff, Alvin, and Reese, David E., Jr., "Defining Mars' atmosphere - A goal for the early missions," Astronautics and Aeronautics, 3, no. 2, 16-21 (Feb. 1965).

TABLE I.- TYPICAL ENERGY BALANCES (percentages)

	Tektite glass (semitransparent) wind tunnel (Fig. 1)	Tektite Earth entry (opaque) (Figs. 3, 4)	Silica glass heat-shield Earth entry (transparent)	Silica glass heat-shield Earth entry (semitransparent)	Teflon wind tunnel (Fig. 5) h_S=2000 Btu/lb p_S=0.34 atm	Teflon Mars entry γ_i=-20° $V_{\infty i}$=7.92 km/sec
Convection in (hot wall)	100.0	100.0	100.0	100.0	100.0	100.0
Heat blocked	2.9	31.9	11.4	11.5	35.4	70.1
(Net convection in)	(97.1)	(68.1)	(88.6)	(88.5)	(64.6)	(29.9)
Net radiation in	-13.3	-10.8	-28.4	-27.6	-4.8	-3.6
Heating and vaporizing	5.2	24.9	21.5	21.2	50.1	23.6
Heating and melting	69.1	27.2	28.6	31.6	0	0
Stored	4.6	6.3	10.4	6.9	9.9	2.8
Error	4.9	-1.1	-0.3	1.2	-0.2	-0.1

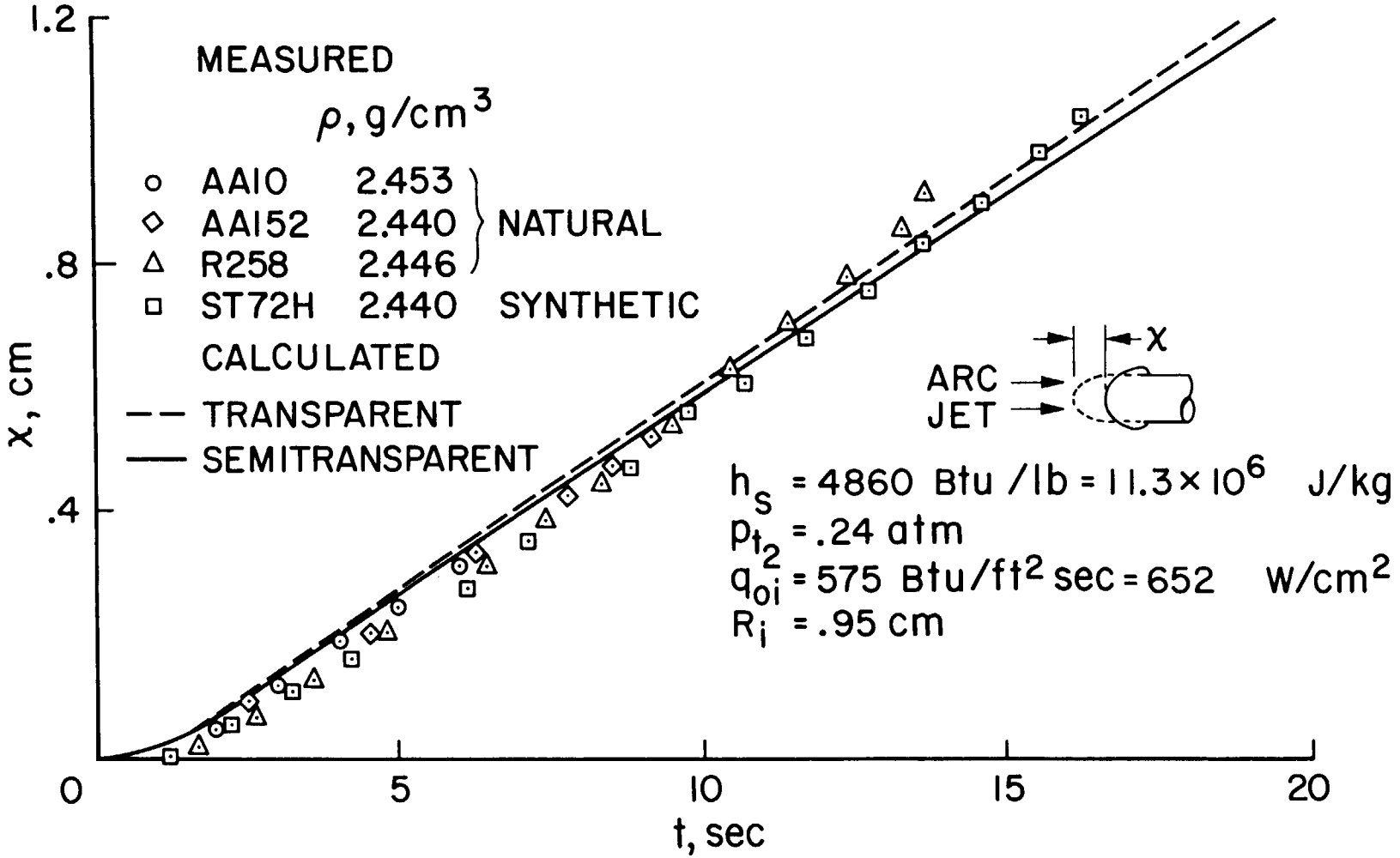

Fig. 1.- Comparison of calculated and measured surface recession of tektite glass in a wind tunnel.

NATIONAL AERONAUTICS AND SPACE ADMINISTRATION
AMES RESEARCH CENTER, MOFFETT FIELD, CALIFORNIA

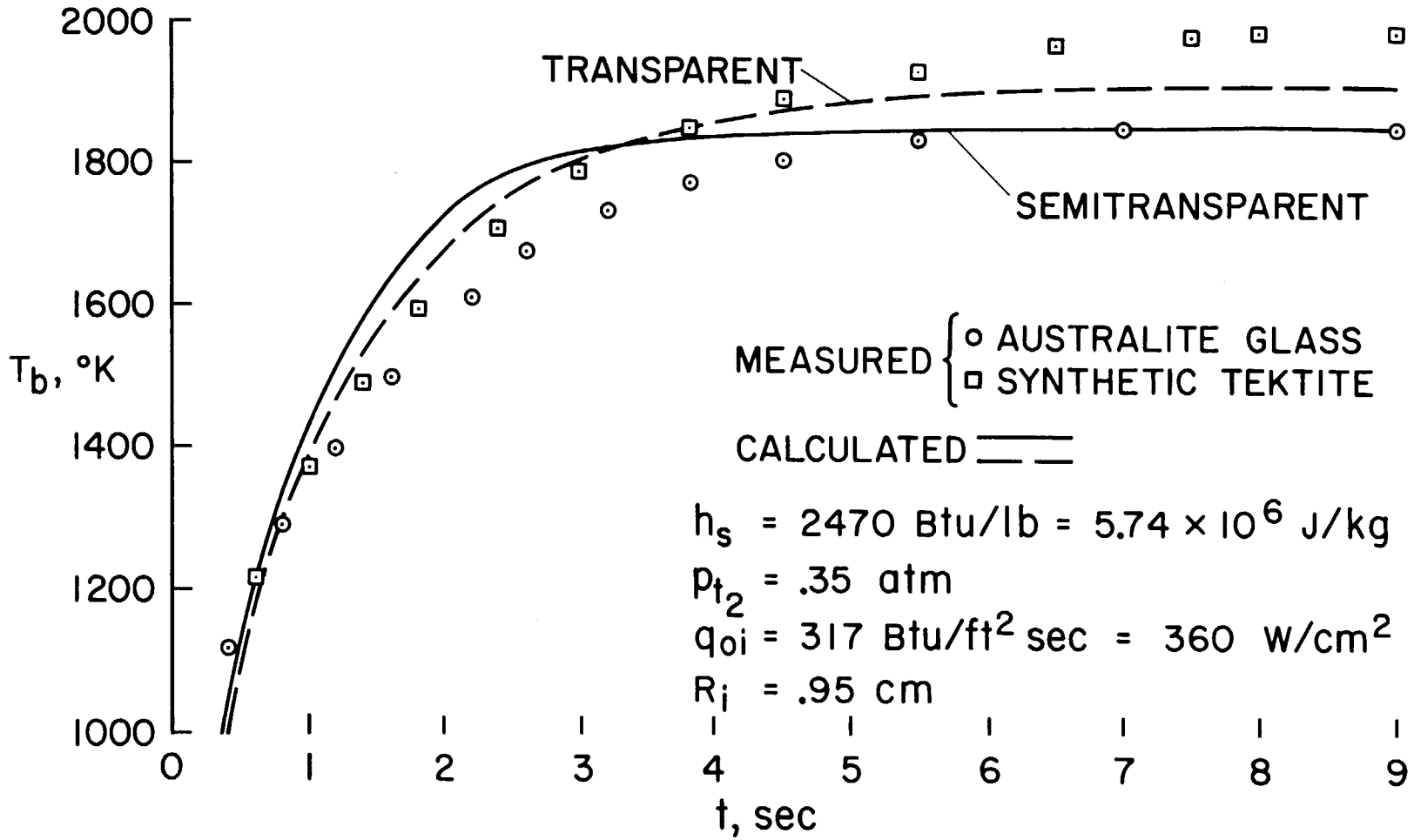

Fig. 2.- Comparison of calculated and measured brightness temperature of tektite glass in a wind tunnel.

NATIONAL AERONAUTICS AND SPACE ADMINISTRATION
AMES RESEARCH CENTER, MOFFETT FIELD, CALIFORNIA

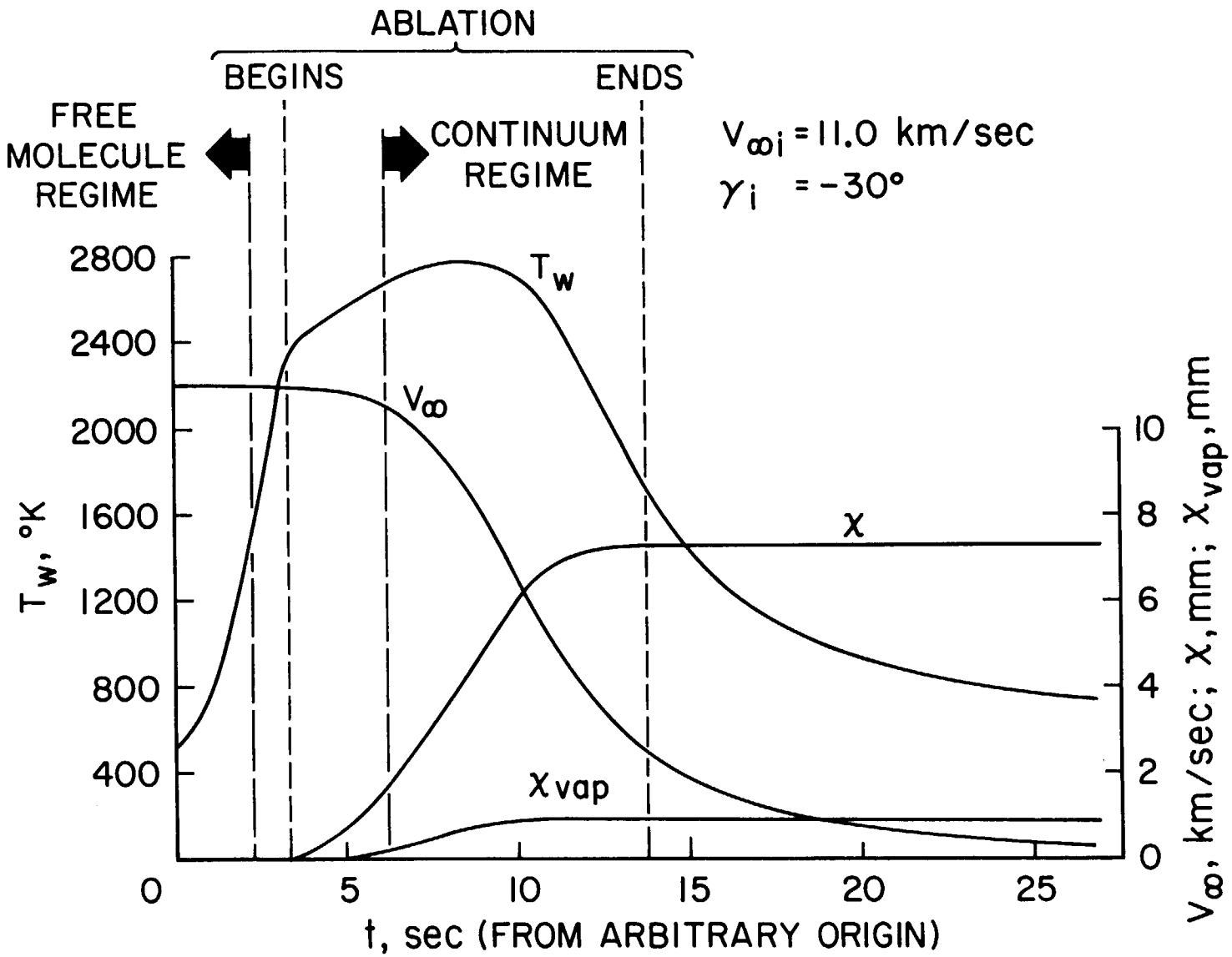

Fig. 3.- Calculated variation of surface temperature, velocity, total ablation, and vaporized ablation for a Victoria australite entering Earth's atmosphere; $V_{\infty i}$ = 11.0 km/sec, γ_i = -30°, R_i = 0.816 cm.

NATIONAL AERONAUTICS AND SPACE ADMINISTRATION
AMES RESEARCH CENTER, MOFFETT FIELD, CALIFORNIA

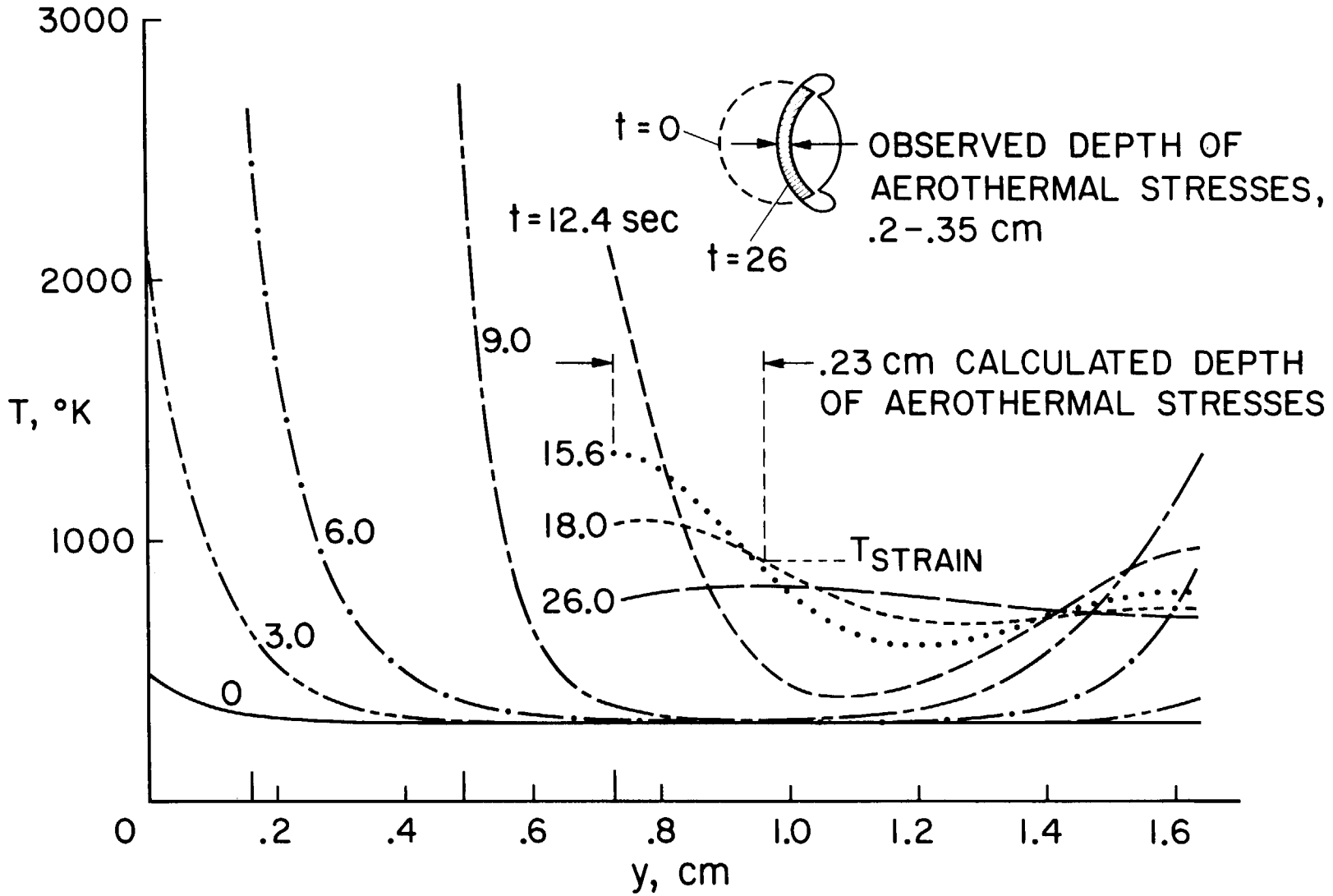

Fig. 4.- Calculated temperature profiles for a Victoria australite entering Earth's atmosphere; $V_{\infty i}$ = 11.0 km/sec, γ_i = -30°, R_i = 0.816 cm.

NATIONAL AERONAUTICS AND SPACE ADMINISTRATION
AMES RESEARCH CENTER, MOFFETT FIELD CALIFORNIA

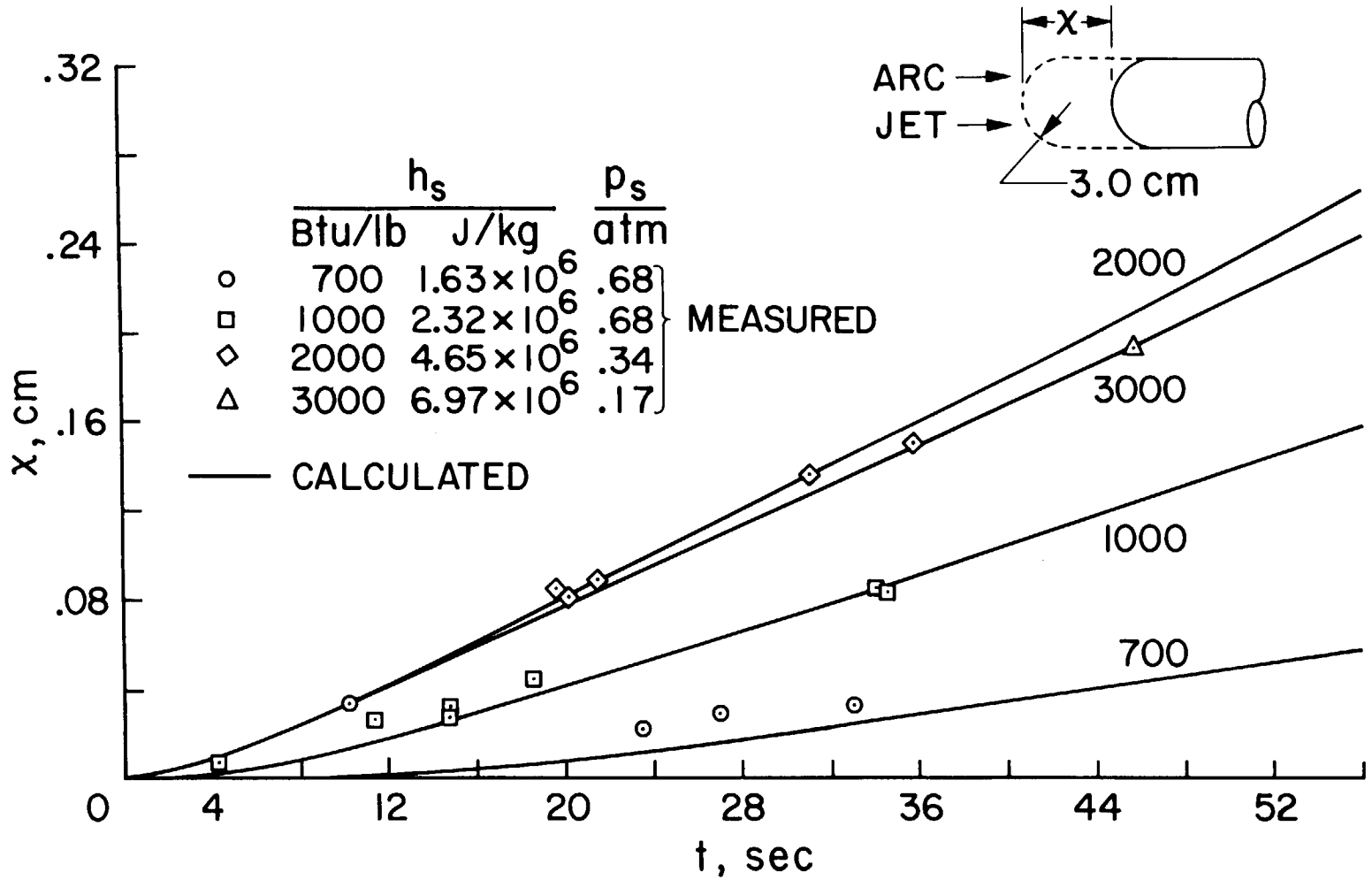

Fig. 5.- Comparison of calculated and measured surface recession of Teflon in wind tunnel.

NATIONAL AERONAUTICS AND SPACE ADMINISTRATION
AMES RESEARCH CENTER, MOFFETT FIELD, CALIFORNIA

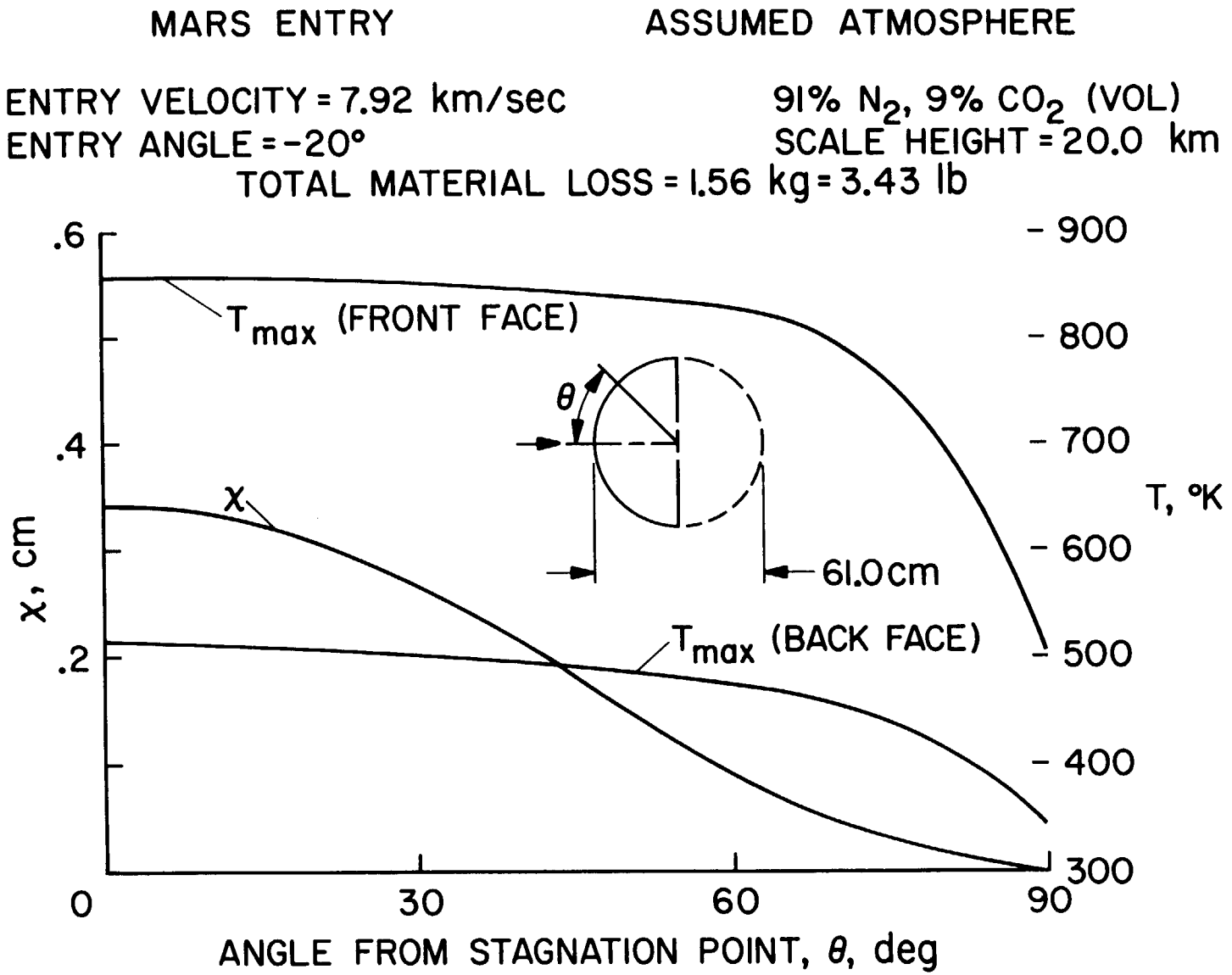

Fig. 6.- Approximate calculation of response of a Teflon heat shield in a Mars entry.

NATIONAL AERONAUTICS AND SPACE ADMINISTRATION
AMES RESEARCH CENTER, MOFFETT FIELD, CALIFORNIA